

Modeling Study of the Formation of Single- and Multiple-Layered Arctic Stratus Clouds

*Q. Zhang
University of Utah
Salt Lake City, Utah*

*K. Stamnes and J. Harrington
Geophysical Institute
University of Alaska
Fairbanks, Alaska*

*O. Lie-Svendsen
Norwegian Defense Research Establishment
Kjeller, Norway*

Introduction

Arctic stratus clouds (ASCs) are a persistent feature in the arctic. They may have an important influence on both the local climate and the global climate. Due to lack of observations, the formation of ASCs and their interactions with radiation are still uncertain. Curry and Herman (1985) suggested that ASCs form as relatively warm and moist air flows into the arctic from lower latitudes and are cooled radiatively and by contact with the colder surface of the sea ice and ocean.

ASCs are often observed with multiple layers. The upper cloud layer or layers are often covered with strong temperature inversion and the lowest layer may reach the surface. Three hypotheses have been proposed to explain the multiple layers of ASCs. The one-dimensional (1-D) turbulence closure-radiative transfer model results of Herman and Goody (1976) supported the idea that solar absorption warms the interior of a surface-based cloud and thereby forms a clear layer between two cloudy layers. Tsay and Jayaweera (1984) proposed that very weak ascent or entrainment forms the upper cloud layer, while the surface cloud layer is an advective fog. McInnes and Curry (1995) suggested a third mechanism that radiative cooling leads initially to the formation of the upper cloud layer near the peak of the preexisting temperature and humidity inversion where radiative cooling is the strongest, while the lower cloud layer is formed by radiative cooling at the base of the upper mixed layer.

In this research we will investigate the formation of ASCs by adopting a 1-D radiative-convective model, which includes detailed cloud microphysical processes. The role of radiative transfer in the cloud formation is discussed. Lie-Svendsen et al. (1999) and Zhang (1999) presented detailed descriptions of the model. The simulations are initiated with a clear atmosphere so that we are able to investigate cloud formation. The initial data for the simulations are based on the observations of

June 28, 1980, over the Beaufort Sea during the Arctic Stratus Experiment. Detailed descriptions of the experiment and analyses of physical properties of the boundary layer were given by Tsay and Jayaweera (1984) and Curry et al. (1988).

The Role of Radiative Transfer on ASCs Formation

To simplify the problem, we will first focus on investigating the formation of a single cloud layer, taken to be the upper cloud layer observed on June 28, 1980. The initial water vapor mixing ratio for the following simulation is shown in Figure 1a. To prevent a cloud layer from forming close to the surface, we reduced the water vapor amount below 0.5 km to levels significantly less than the observed ones. The water vapor mixing ratio is 5.1 g/kg between 0.5 km and 1.2 km altitudes. The relative humidity is about 80%. The water vapor content decreases significantly with height between 1.2 km and 1.3 km, which is in agreement with the observations. This humidity profile yields the dew point temperature profile shown by the dashed line in Figure 1b. The initial temperature decreases with height by a constant lapse rate of 1.8 K/km. The difference between the initial temperature and the dew point temperature is almost constant and is about 2 K between 0.5 km and 1.2 km. Therefore, the cooling required to form a cloud is the same at all levels between 0.5 km and 1.2 km. The surface temperature is held constant at 273.15 K. The diurnal cycle of solar radiation is not included in the simulations to simplify the problem. A fixed solar zenith angle is adopted.

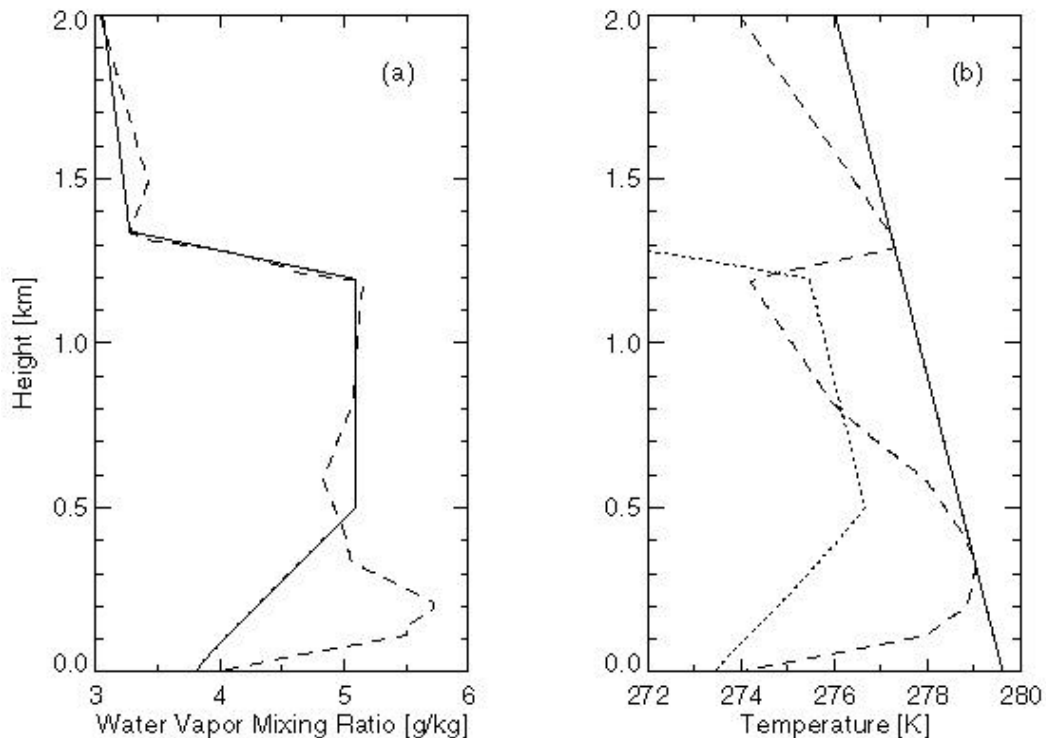


Figure 1. (a) Initial water vapor mixing ratio (g/kg); (b) initial temperature (K). Solid lines are the initial data for simulation. Dashed lines are the observation. The dotted line in the left panel is dew point temperature.

With the initial conditions specified above, the model is integrated forward in time for 35 hours. A single cloud layer appears between 0.8 km and 1.2 km (Figure 2a). This cloud layer initially forms at 30.5 model hours at 1.18 km altitude, and it develops rapidly once it has formed initially. Figure 2 also shows the vertical distribution of cloud droplet density and equivalent radius.

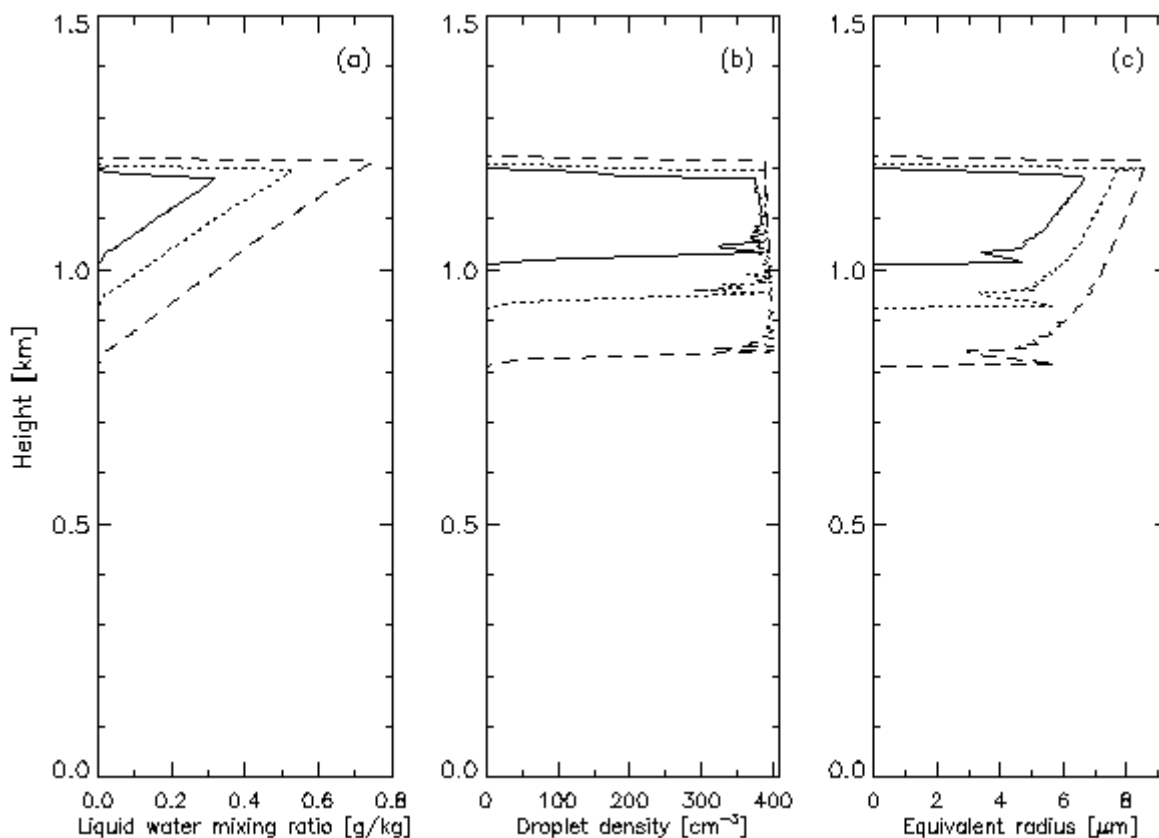


Figure 2. (a) Liquid water mixing ratio (g/kg); (b) droplet density (cm⁻³); (c) equivalent radius (μm). Solid, dotted, and dashed lines correspond respectively to 1.5, 2.5, and 4.5 hours after initial cloud formation.

We now discuss how the cloud forms (or how the water vapor condensation occurs) in the simulation. The dew point temperature is the atmospheric temperature at which water vapor condensation occurs. The dew point temperature profile has not changed much during the simulation since there is only a very slight change in the water vapor profile due to vertical mixing before the initial cloud formation (not shown) and the atmospheric pressure is kept constant during the simulation. For condensation to occur, the atmospheric temperature must decrease to the dew point value. Figure 3 shows how the temperature evolves with time during the simulation. Before the cloud forms, a large temperature decrease occurs near the surface below 0.3 km because the surface temperature is much lower than the atmospheric temperature. The temperature decreases slowly between 0.3 km and 1.2 km at a rate of only about -0.07 K/hour. Near 1.2 km, where a larger water vapor gradient exists, the temperature decrease is somewhat larger than in adjacent layers. This gives rise to a small temperature inversion around this height after 14 model hours.

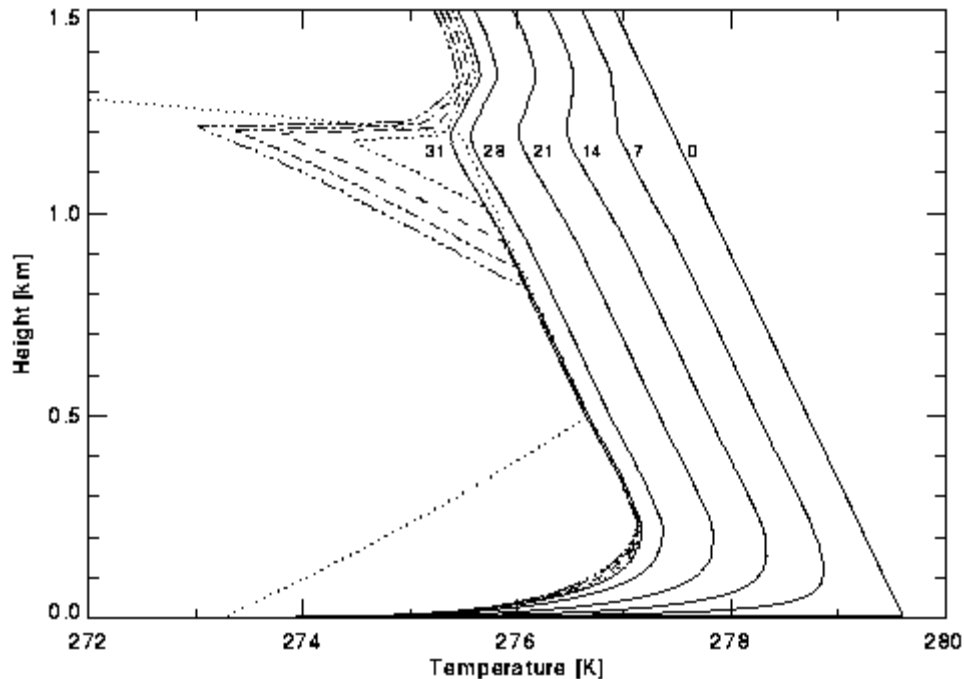


Figure 3. Temperature profiles. Dotted, dashed, dashed-dotted, and dashed-dotted-dotted lines represent profiles at 32, 33, 34, and 35 model hours, respectively. The heavy dotted line is the dew point temperature.

The temperature continues to decrease throughout the atmosphere during the simulation. It first reaches the dew point temperature (the heavy dotted line in Figure 3) at about 1.17 km at 30.5 model hours. Water vapor condensation then occurs and the cloud starts forming at this height. After the initial cloud formation, the temperature decreases very fast in the cloud layer. Such strong temperature decrease causes considerable water vapor condensation and the cloud liquid water increases significantly with time.

Radiative cooling is a significant process in the model that may lead to the temperature decrease before cloud formation since vertical mixing is weak at that period. Figure 4 shows radiative warming/cooling rates before the cloud forms (at 7, 14, 21, and 28 model hours, respectively). There are three peaks in the vertical profile of the infrared cooling rate. Strong infrared radiative cooling occurs near the ground because the surface temperature is much lower than the atmospheric temperature. Two other peaks appear at about 0.5 km and 1.2 km where significant water vapor gradients appear (Figure 1a). The absolute magnitude of the peaks decreases with time. This may be explained by the changes in the temperature profiles as the temperature inversion develops. Also, the vertical mixing processes may cause the water vapor to become more uniformly distributed with height.

The solar warming rate does not vary with time since the solar zenith angle was fixed in this simulation. It is much smaller than the infrared cooling rate (only about 10% of the infrared cooling). There is a peak at 1.18 km in the solar warming rate. This peak coincides with the water vapor gradient.

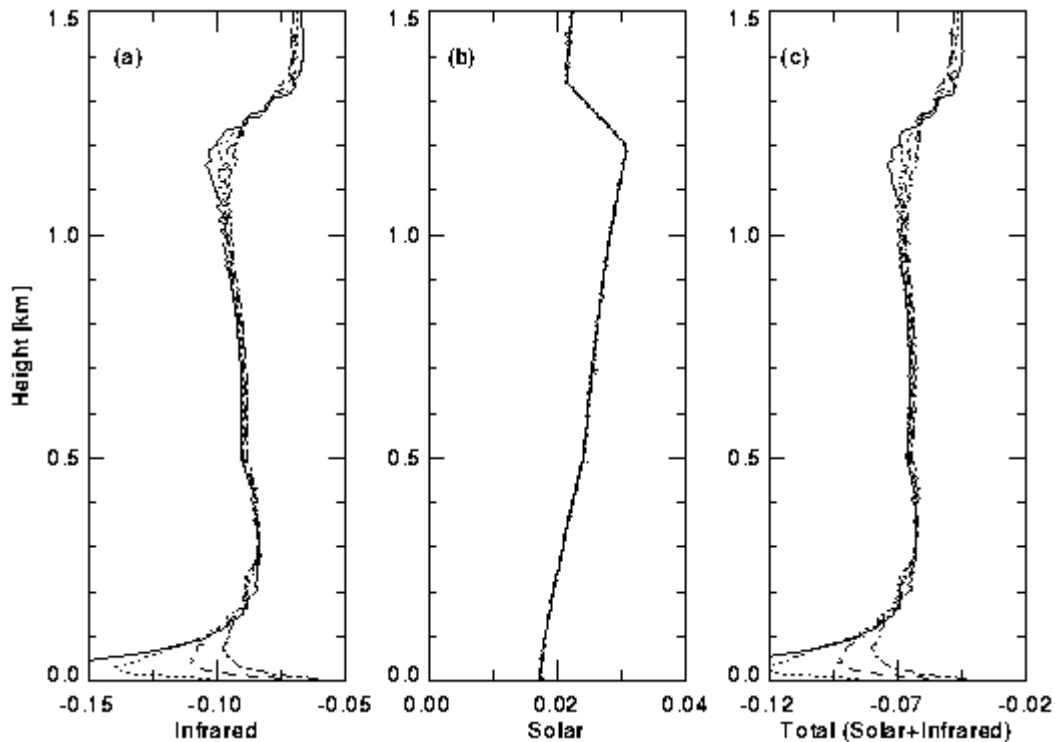


Figure 4. Radiative warming/cooling rates before the cloud forms. Solid, dotted, dashed, and dashed-dotted lines show profiles at 7, 14, 21, and 28 model hours, respectively. Unit is K/hour. (a) infrared; (b) solar; (c) total (infrared + solar).

The total (solar and infrared) radiative effect is negative. Thus, there is a net cooling that will cause a temperature decrease. The total radiative warming/cooling rates range from -0.025 K/hour to -0.08 K/hour between 0.3 km and 1.5 km. The similar appearance of the total and infrared warming/cooling rate profiles suggests that the infrared radiative cooling causes the decrease in temperature. Also, the changes over time in total radiative warming/cooling rates are similar to those of the infrared cooling rates. The total radiative cooling rate is close to the rate of temperature decrease, suggesting that primarily the radiative cooling causes the temperature decrease.

There are three peaks also in the total radiative warming/cooling rate appearing at the same heights as those in the infrared cooling rate. The peak at about 1.2 km causes the temperature at that height to decrease more than at other heights between 0.3 km and 1.5 km. This temperature decrease eventually leads to the initial cloud formation at around that height. The somewhat larger cooling rate at about 1.2 km corresponds to the large water vapor gradient there. This cooling rate leads to a small temperature inversion at this height after 14 model hours, and to the initial cloud formation at 30.5 model hours. The appearance of the temperature inversion may cause the infrared cooling rate to decrease slightly at that height, which partly offsets the initial radiative cooling effect. However, the above analyses suggest that the initial condensation of water vapor at 1.2 km is due to the continual

temperature decrease caused by the enhanced infrared radiative cooling associated with the significant moisture gradient at this level. The cloud formation depends somewhat on the vertical profile of humidity.

Five sensitivity simulations are conducted (Figure 5) to further investigate the effect of humidity gradients on radiative transfer and thus on cloud formation. The initial water vapor mixing ratios adopted for these five simulations are shown in Figure 5a. Below 1 km the initial water vapor content of the five simulations are taken to be the same; they are different only between 1 km and 3 km. An abrupt change in humidity is assumed to occur at the 1-km level. The humidity gradient at the 1-km level influences the profiles of both solar and infrared warming/cooling rates, and thus the total radiative warming/cooling rates. A negative humidity gradient (humidity decreases with height at the 1-km level) yields solar warming and infrared cooling rates that are stronger below 1-km height than the above,

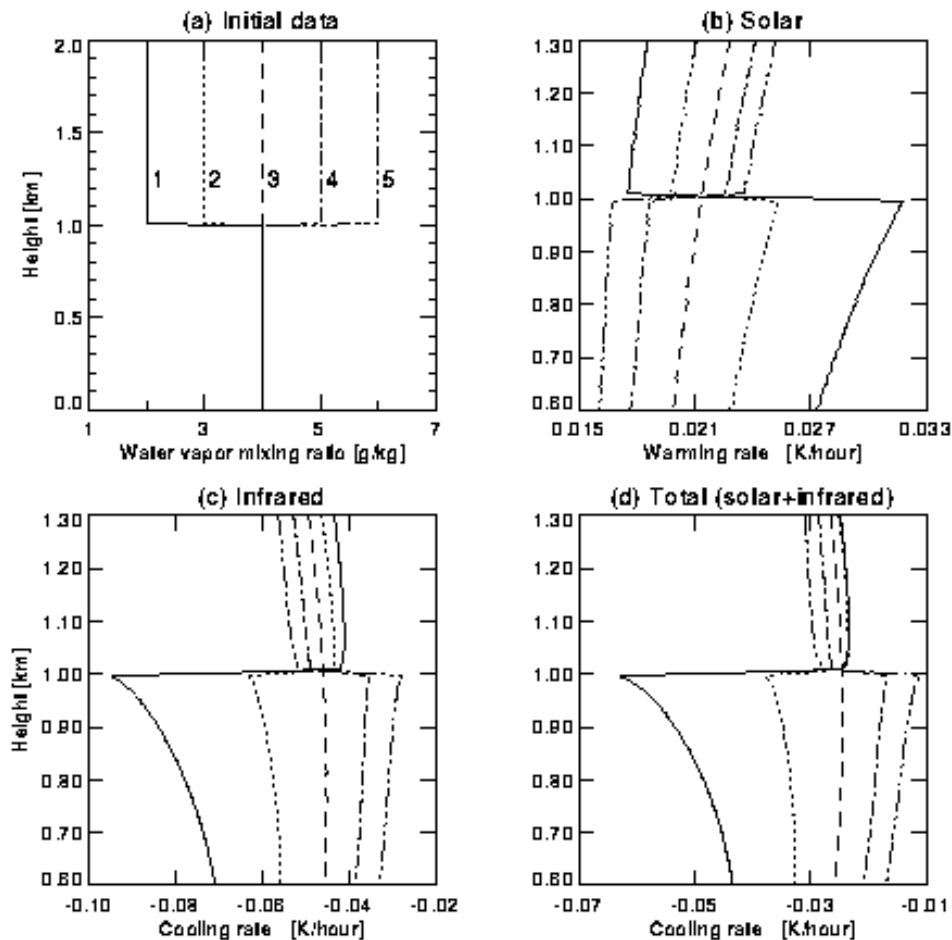


Figure 5. The effect of the water vapor gradient on the radiative transfer. (a) Initial water vapor mixing ratio; (b) solar only; (c) infrared only; (d) total (solar + infrared). Solid, dotted, dashed, dashed-dotted, and dashed-dotted-dotted lines correspond to the different humidity profiles specified in (a), corresponding to a jump in the water vapor mixing ratio of -2 , -1 , 0 , 1 , and 2 g/kg, respectively, across the 1 km level.

while positive humidity gradient (humidity increases with height at 1-km level) yields solar warming and infrared cooling rates that are weaker below the 1-km level than the above. Peaks appear at the 0.995-km level in the solar and infrared warming/cooling rates, and thus in the total radiative warming/cooling rates. The larger the negative humidity gradient, the larger are the peaks in radiative warming/cooling rates. This suggests that a certain critical humidity gradient is required in order for the cloud to form.

The Formation of Two Cloud Layers

Several simulations are made to investigate the formation of multiple-layered ASCs. Those simulations are initialized with the data designed according to the observation of June 28, 1980. The results suggest that radiative cooling plays a key role during the initial stage of the cloud layers formation (Zhang et al. 1998; Zhang 1999). Both the two-cloud layers may form due to continual temperature decrease caused by radiative cooling that is determined by the vertical distribution of humidity.

Acknowledgments

This research was supported by the U.S. Department of Energy through contract 091574-A-Q1 to the University of Alaska, Fairbanks.

References

- Curry, J. A., and G. F. Herman, 1985: Relationships between large-scale heat and moisture budgets and the occurrence of Arctic stratus clouds. *Mon. Wea. Rev.*, **113**, 1441-1457.
- Curry, J. A., E. E. Ebert, and G. F. Herman, 1988: Mean and turbulence structure of the summertime Arctic cloudy boundary layer. *Quart. J. Roy. Met. Soc.*, **114**, 715-746.
- Herman, G., and R. Goody, 1976: Formation and persistence of summertime Arctic stratus clouds. *J. Atmos. Sci.*, **33**, 1537-1553.
- Lie-Svendsen, O., Q. Zhang, J. Delamere, and K. Stamnes, 1999: The role of radiation and microphysics in the formation of Arctic Stratus Clouds. *Tellus*. Submitted.
- McInnes, K., and J. A. Curry, 1995: Modeling the mean and turbulent structure of the arctic summertime cloudy boundary layer. *Bound. Layer Meteor.*, **73**, 125-143.
- Tsay, S.-C., and K. Jayaweera, 1984: Physical characteristics of Arctic stratus clouds. *J. Climate Appl. Meteor.*, **23**, 584-596.
- Zhang, Q., K. Stamnes, and O. Lie-Svendsen, 1998: Formation of Arctic stratus clouds: comparison of model predictions with observed cloud structure. In *Proceedings of the Eighth Atmospheric Radiation Measurement (ARM) Science Team Meeting*, DOE/ER-0738, pp. 853-856. U.S. Department of Energy, Washington, D.C.

Zhang, Q., 1999: Modeling of Arctic stratus cloud formation and the maintenance of the cloud Arctic boundary layer. *Ph.D. Thesis*. University of Alaska, Fairbanks, 198 p.